Snapshot polarization-sensitive plug-in optical module for a Fourier-domain optical coherence tomography system

Manuel J. Marques[a,*], Sylvain Rivet[b], Adrian Bradu[a], and Adrian Podoleanu[a]

[a]Applied Optics Group, School of Physical Sciences, University of Kent, Canterbury CT2 7NH, United Kingdom.

[b]Laboratoire d'optique et de magnétisme EA938, IBSAM, Université de Bretagne Occidentale, 6 avenue Le Gorgeu, C.S. 93837, 29238 Brest Cedex 3, France

[*]M.J.Marques@kent.ac.uk

ABSTRACT

In this communication, we present a proof-of-concept polarization-sensitive Optical Coherence Tomography (PS-OCT) which can be used to characterize the retardance and the axis orientation of a linear birefringent sample. This module configuration is an improvement from our previous work[1,2] since it encodes the two polarization channels on the optical path difference, effectively carrying out the polarization measurements simultaneously (snapshot measurement), whilst retaining all the advantages (namely the insensitivity to environmental parameters when using SM fibers) of these two previous configurations. Further progress consists in employing Master Slave OCT technology,[3] which is used to automatically compensate for the dispersion mismatch introduced by the elements in the module. This is essential given the encoding of the polarization states on two different optical path lengths, each of them having dissimilar dispersive properties. By utilizing this method instead of the commonly used re-linearization and numerical dispersion compensation methods an improvement in terms of the calculation time required can be achieved.

Keywords: polarization-sensitive OCT, polarimetry, fiber-based system

1. INTRODUCTION

Frequency-domain OCT methods (both spectrometer- and swept-source-based) have been extensively used over the past decade to image translucent structures.[4] Polarization-sensitive optical coherence tomography (PS-OCT) methods emerged as early as 1992,[5] evolving from bulk-based to more compact fiber-based designs. These systems are useful in medical OCT applications due to the link between polarization properties and the health state of biological tissues. In non-destructive testing, PS-OCT also provides birefringence information, which is useful in assessing the mechanical properties of the structures evaluated.

Due to their versatility, easy alignment, compact size and the need for single spatial mode selection, fiber-based systems are used in OCT practice.[6] However, external factors (such as temperature and mechanical stress) affect the birefringence of single-mode fibers (SMFs) used in OCT systems, inducing disturbances[7] to the measured polarization.

One way to avoid the influence of these external factors and their corresponding disturbances is to perform the polarization selection before the collecting fiber, which was firstly demonstrated by Roth *et al.* in 2001.[8] Our approach[1] reported in 2015 follows the same philosophy, while also ensuring a circular polarization state in the imaging beam, which minimizes the number of measurements required for a full characterization of polarization. We have followed up on this approach by reporting[2] on a configuration which mitigates the drawbacks from the first configuration, namely the power losses stemming from the sample arm design. However, both configurations rely on active devices to perform the polarization measurements and they are sequential by design, which requires additional strategies if the measurement of the optical axis orientation is desired.

In this communication, we report[9] on a novel approach, which overcomes the main limitations of the two previous configurations. This approach is based on an in-line passive optical module (POM) which contains only passive optical elements. This module can be placed in the free space portion of any frequency-domain

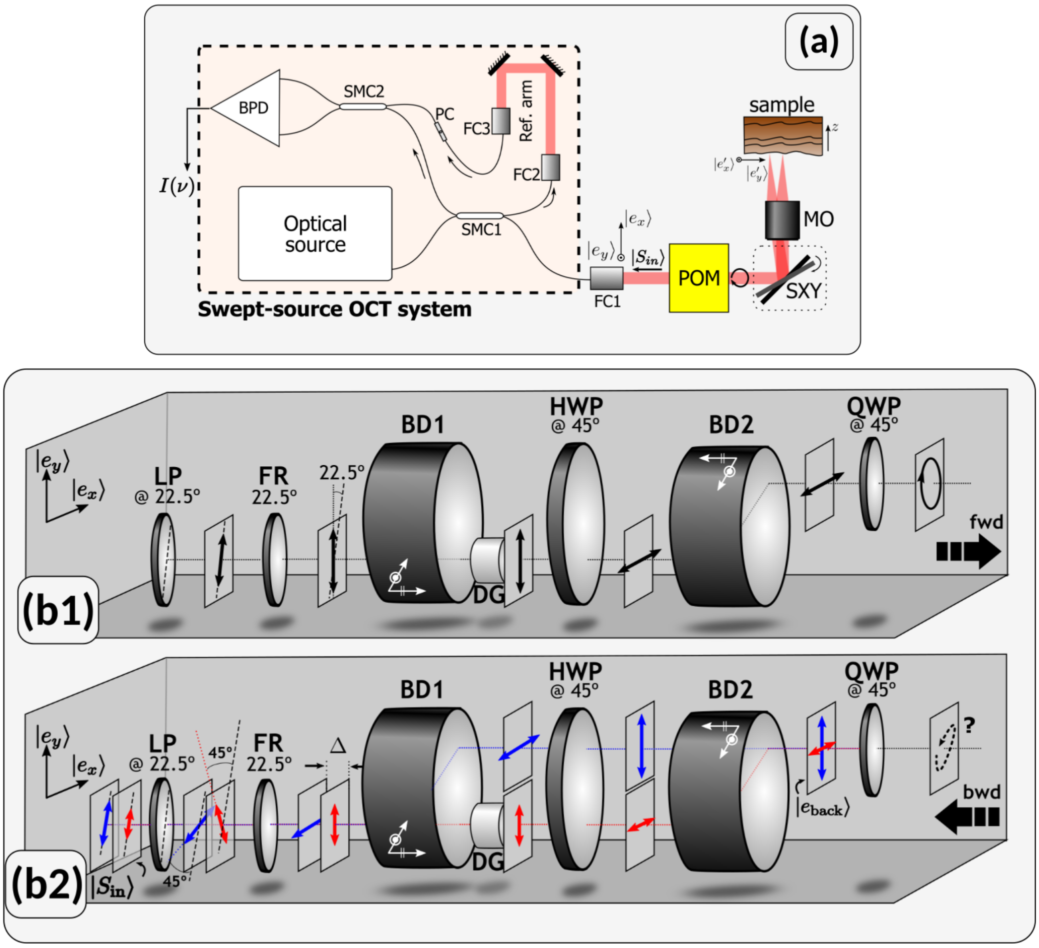

Figure 1. (a) schematic diagram of the POM when installed in a swept-source OCT system. (b1) detail of the POM illustrating the evolution of the polarization state of the illuminating beam; (b2) detail of the POM illustrating the evolution of the polarization state of the light collected from the sample. The key to the diagram can be found in our previous publication.[9]

OCT system (as shown in Fig. 1 (a)), and is schematically represented in Figs. 1 (b1)-(b2) for the forward (illuminating) and backward (collection) propagation paths, respectively.

The operation of this module has been fully detailed in our recent publication.[9] Briefly, light arriving at the POM in forward propagation (Fig. 1 (b1)) travels through one of the possible paths created by the beam displacers (BD1-2). The quarter-wave plate placed just before the scanners SXY ensures the sample is illuminated with circularly polarized light. On the backward propagation path (Fig. 1 (b2)) the unknown polarisation state returning from the sample is decomposed in its two orthogonal components, which are then separated by BD2. The presence of a piece of dispersion glass (DG) in one of the paths ensures that the two beams with orthogonal polarization states travel different optical path lengths, thus allocating them to separate frequency regions of the detected channeled spectra. In this way, the two polarization channels (denoted as $\hat{A}_1$ and $\hat{A}_2$ in our previous publication[9]) can be read simultaneously, while preserving all the other advantages presented in the two previous configurations.[1,2] The two polarization parameters, the one-pass retardance φ and fast axis orientation θ can then be determined for a given depth z_0 using the expressions described in Ref.[9] :

$$\varphi(z_0) = \arctan\left[\left|\frac{\hat{A}_2(z_0)}{\hat{A}_1(z_0)}\right|\right], \tag{1}$$

and

$$\theta(z_0) = \arg\left[\frac{\hat{A}_2(z_0)}{\hat{A}_1(z_0)}\right]/2 + m\pi, \tag{2}$$

with $\varphi(z_0) \in [0, 90]$ degrees, $\theta \in [-90, 90]$ degrees and arg denotes the argument of the complex number $\hat{A}_2(z_0)/\hat{A}_1(z_0)$.

The introduction of the POM in the set-up creates unbalanced dispersion not only between the sample and reference arms, but also between both paths within the POM due to the presence of the dispersive glass block DG. Using conventional FFT-based methods would require either hardware- or software-based depth-dependent dispersion compensation; therefore, we have employed the complex Master-Slave method.[3] At the calibration stage (labelled 'Master stage' in the literature[3]), a mirror is used as an object and the resulting spectra are acquired for either channel, and then used to calculate the two sets of masks, one for each channel (vertical and horizontal polarization components), as depicted in the diagram in Figure 2. After performing the comparison step of the incoming signal from the sample with the two sets of complex masks (the 'Slave' stage in the literature), the complex A-scan is recovered for both channels and Equations (1) and (2) can be used to obtain the polarimetric measurements of the sample.

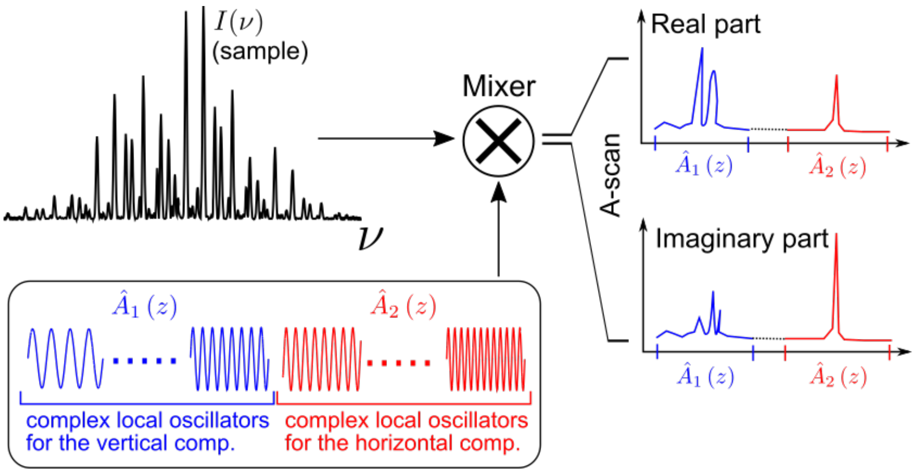

Figure 2. Schematic representation (derived from Rivet *et al.*[9]) of the CMS procedure mixing two sets of digital local oscillators, which corresponds to the two orthogonal polarization channels (labeled "vertical"/$\hat{A}_1$ and "horizontal"/$\hat{A}_2$ in this diagram), with the channeled spectra $I(\nu)$ obtained when the sample is imaged.

2. PERFORMANCE CHARACTERIZATION OF THE MODULE

To validate the operation of the POM, a series of measurements from a calibrated sample, a Berek compensator (Newport model 5540) were performed while varying the retardance setting of the Berek (the "indicator" setting J, which can be related to the retardance as described in[10]) as well as the orientation of the device in relation to the incoming beam.

It can be observed from the plot in Fig. 3 (a) that the retardance measurements present very little variability with the orientation of the compensator. This was not the case with our first reported PS-OCT system,[1] where the active polarization rotator employed in the system introduced a measurement error which was orientation-dependent.

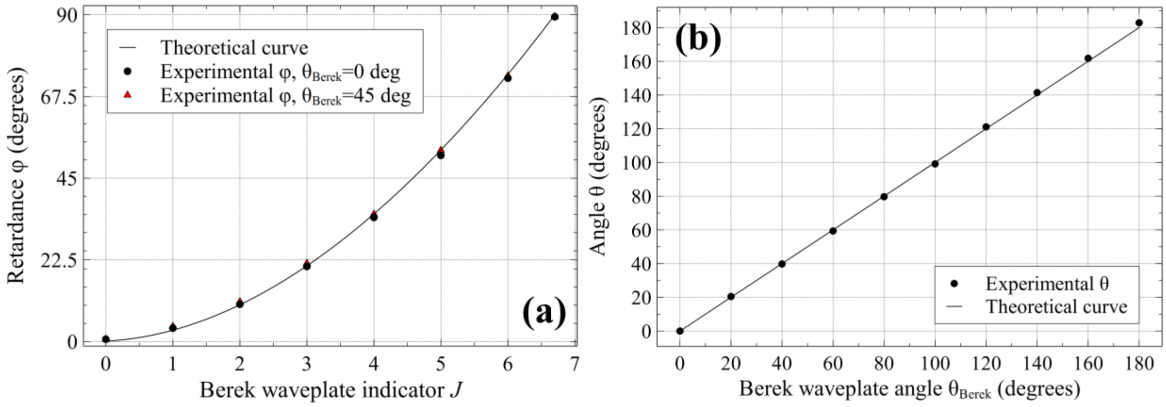

Figure 3. Validation of the POM with the Berek compensator. **(a)** measurements of the retardance introduced by the Berek versus the position of its indicator J. The black line corresponds to the theoretical values of the retardance computed as a function of J, and between the two sets of experimental data (black dots and red triangles) the Berek compensator has been rotated by 45 degrees around the propagation axis. **(b)** measurement of the Berek angle orientation using Eq. (2) versus the orientation of the Berek compensator θ_{Berek} read on the rotation stage.

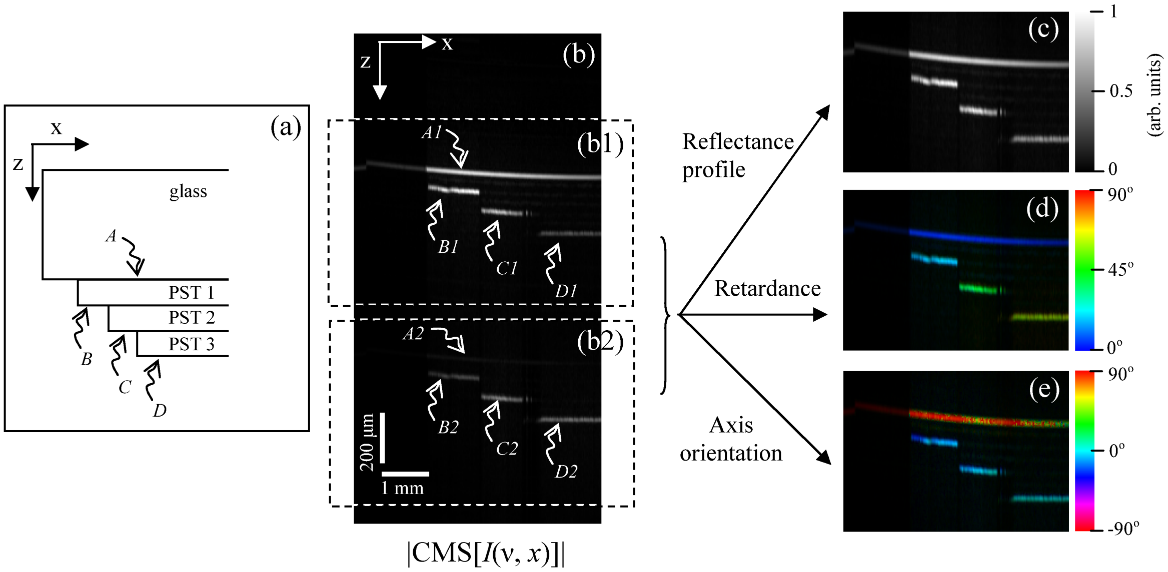

Figure 4. Characterization of the POM using a birefringent phantom, consisting on several layers of pressure-sensitive tape mounted over a glass slide. (a) schematic representation of the birefrigent phantom; (b) the raw B-scan obtained, containing the two polarization channels multiplexed in OPD; (c) reconstructed reflectance profile; (d) net retardance profile; (e) net axis orientation profile. More details in Rivet *et al.*[9]

Additionally, to illustrate the operation of the POM within an imaging OCT system, a phantom made from several specular layers was imaged. This was assembled by using a 1.5 mm piece of anti-reflection coated glass, onto which 3 strips of pressure-sensitive tape (PST, transparent adhesive tape) were laid in cascade, as shown in Fig. 4(a). The PST exhibits linear retardance. The different interfaces within the sample are labelled as A, B, C and D respectively.

The two polarization components from the light returning from the sample are represented at separate depth ranges in the B-scan in Fig. 4 (b).

By computing the absolute value of the two components, one can obtain the reflectance profile of the sample, as represented in Fig. 4 (c). This is the information one typically acquires with a standard OCT system. In addition to that, by computing the ratio of the two channels as described in the PSOCT literature (for a single input-state system) one can obtain both the sample retardance and the axis orientation, as shown in Figs. 4 (d)-(e).

3. FINAL REMARKS

In this communication, we present a passive optical module capable of introducing polarization-sensitive capabilities to any frequency-domain OCT system. We have demonstrated said module by coupling it to a swept-source based OCT system and characterizing it by using a birefringent phantom.

Similarly to the systems we previously presented,[1,2] this module enables use of single-mode fibers whilst avoiding the dependency on environmental parameters introduced by them. Additionally, by encoding the two polarization channels in the OPD, the module allows for simultaneous measurement of the two polarization channels, avoiding the need for special strategies to determine the optical axis orientation such as the ones described in our previous publication.[2]

In the conference, more details will be presented on how this module operates and how the CMS method is beneficial for its simplified operation; not only it somewhat simplifies the dispersion compensation procedure, but there are also a performance benefit in relation to the FFT method when re-linearization is necessary.[11]

ACKNOWLEDGMENTS

S. Rivet acknowledges the Marie-Curie Intra-European Fellowship for Career Development, No. 625509. M. J. Marques, A. Bradu, and A. Podoleanu acknowledge the support of the Engineering and Physical Sciences Research Council (EPSRC) through the '*REBOT*' project EP/N019229/1. A. Bradu, M. J. Marques and A. Podoleanu were partially supported by the European Research Council (ERC) under the European Union's Seventh Framework Programme, Advanced Grant agreement '*COGATIMABIO*', 249889. A. Podoleanu is also supported by the European Industrial Doctorate *UBAPHODESA*, FP7-PEOPLE-2013-ITN 607627, ERC '*ADASMART*' 754695, Royal Society Wolfson Research Merit Award and by the NIHR Biomedical Research Centre at Moorfields Eye Hospital NHS Foundation Trust and UCL Institute of Ophthalmology.

REFERENCES

[1] Marques, M. J., Rivet, S., Bradu, A., and Podoleanu, A., "Polarization-sensitive optical coherence tomography system tolerant to fiber disturbances using a line camera," *Optics letters* **40**(16), 3858–3861 (2015).

[2] Rivet, S., Marques, M. J., Bradu, A., and Podoleanu, A., "Optical module to extend any fourier-domain optical coherence tomography system into a polarisation-sensitive system," *Journal of Optics* **18**(6), 065607 (2016).

[3] Rivet, S., Maria, M., Bradu, A., Feuchter, T., Leick, L., and Podoleanu, A., "Complex master slave interferometry," *Optics express* **24**(3), 2885–2904 (2016).

[4] Drexler, W., Liu, M., Kumar, A., Kamali, T., Unterhuber, A., and Leitgeb, R. A., "Optical coherence tomography today: speed, contrast, and multimodality," *Journal of biomedical optics* **19**(7), 071412–071412 (2014).

[5] Hee, M. R., Swanson, E. A., Fujimoto, J. G., and Huang, D., "Polarization-sensitive low-coherence reflectometer for birefringence characterization and ranging," *JOSA B* **9**(6), 903–908 (1992).

[6] Ding, Z., Liang, C.-P., Tang, Q., and Chen, Y., "Quantitative single-mode fiber based ps-oct with single input polarization state using mueller matrix," *Biomedical optics express* **6**(5), 1828–1843 (2015).

[7] Rashleigh, S. C., "Acoustic sensing with a single coiled monomode fiber," *Optics Letters* **5**(9), 392–394 (1980).

[8] Roth, J. E., Kozak, J. A., Yazdanfar, S., Rollins, A. M., and Izatt, J. A., "Simplified method for polarization-sensitive optical coherence tomography," *Optics Letters* **26**(14), 1069–1071 (2001).

[9] Rivet, S., Marques, M. J., Bradu, A., and Podoleanu, A., "Passive optical module for polarization-sensitive optical coherence tomography systems," *Opt. Express* **25**, 14533–14544 (Jun 2017).

[10] Newport Corporation, *The Berek Polarization Compensator Model 5540* (2012).

[11] Bradu, A., Rivet, S., and Podoleanu, A., "Master/slave interferometry–ideal tool for coherence revival swept source optical coherence tomography," *Biomedical Optics Express* **7**(7), 2453–2468 (2016).